Electronic Supplementary Material (ESI) for Materials Chemistry Frontiers.

Supporting Information

Necklace-like $NiCo_2O_4$@carbon composite nanofibers derived from metal-organic framework compounds for high rate lithium storage

Zhiwen Long[a,1], Rongrong Li[a,1], Zixin Dai[a], Chu Shi[a], Caiqin Wu[a], Qufu Wei[a], Hui Qiao[a,*], Keliang Wang[b,*], Ke Liu[c,*]

[a] Key Laboratory of Eco-textiles, Ministry of Education, Jiangnan University, Wuxi 214122, China

[b] Fraunhofer USA, Inc., Center for Midwest, Division for Coatings and Diamond Technologies, Michigan State University, East Lansing, MI 48824, USA

[c] Hubei Key Laboratory of Low Dimensional Optoelectronic Material and Devices, Hubei University of Arts and Science, Xiangyang, Hubei 441053, China

[1] Authors Zhiwen Long and Rongrong Li contributed equally.

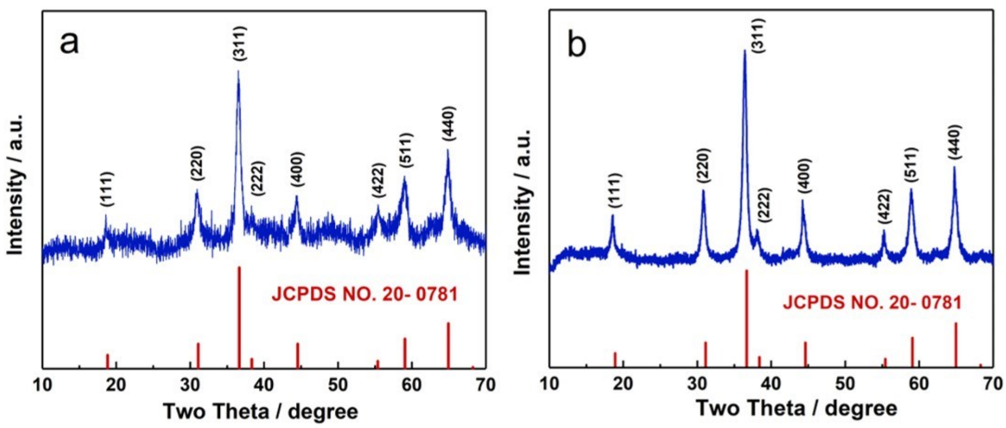

* Corresponding author. Tel/Fax: +86-510-8591-2009
E-mail: huiqiao@jiangnan.edu.cn (H. Qiao), klwang@msu.edu (K. L. Wang), liuk1981@126.com (K. Liu)

Fig. S1 XRD patterns of NCO@C-82 (a) and NCO@C-88 (b) composite nanofibers

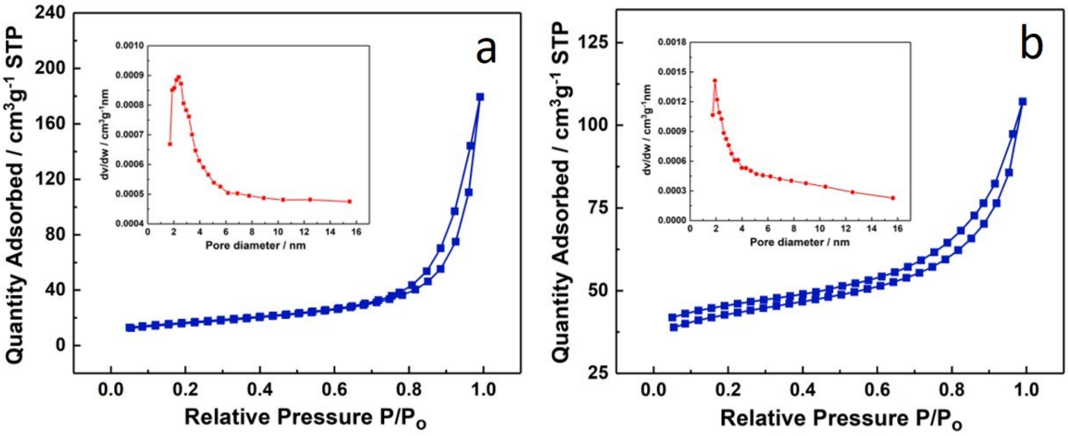

Fig. S2 Specific surface areas of NCO@C-82 (a) and NCO@C-88 (b) composite nanofibers

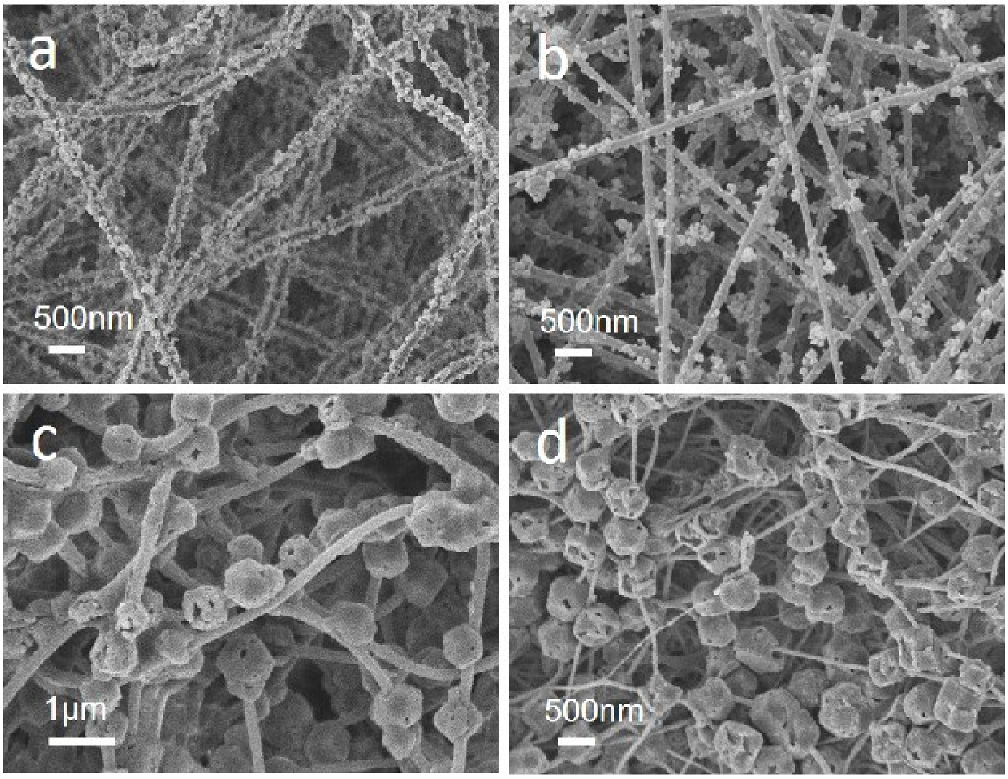

Fig. S3 SEM images of ZIF/PAN-Ni-82 (a), NCO@C-82 (b), ZIF/PAN-Ni-88 (c) and NCO@C-88 (d) composite nanofibers.

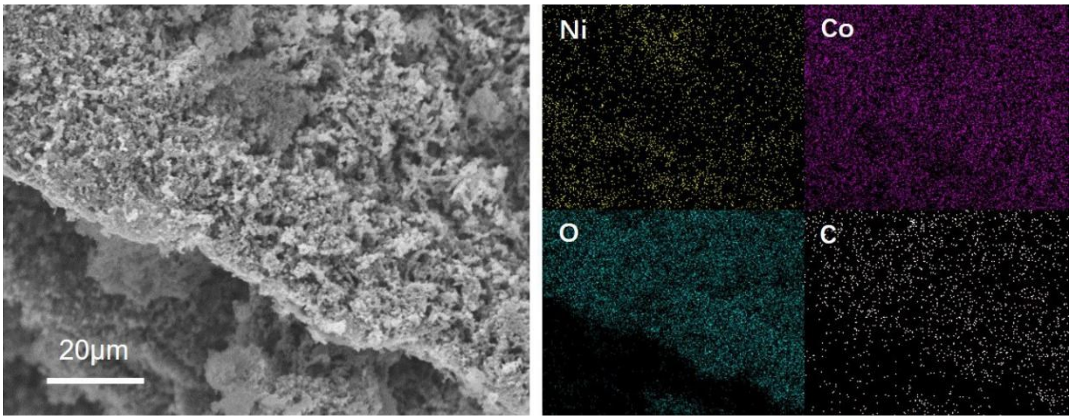

Fig. S4 EDS elemental mapping of Ni, Co, O and C for NCO@C-86 nanofibers.

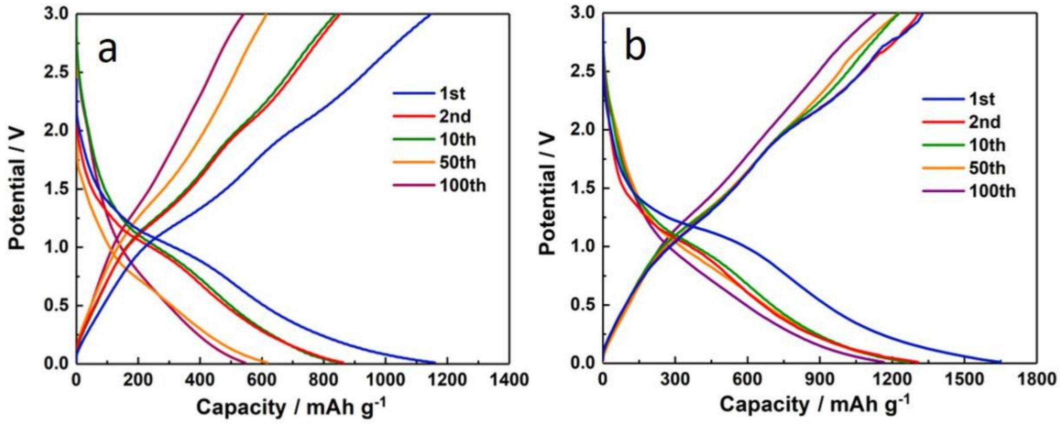

Fig. S5 Charge-discharge curves of NCO@C-82 (a) and NCO@C-88 (b) composite nanofibers

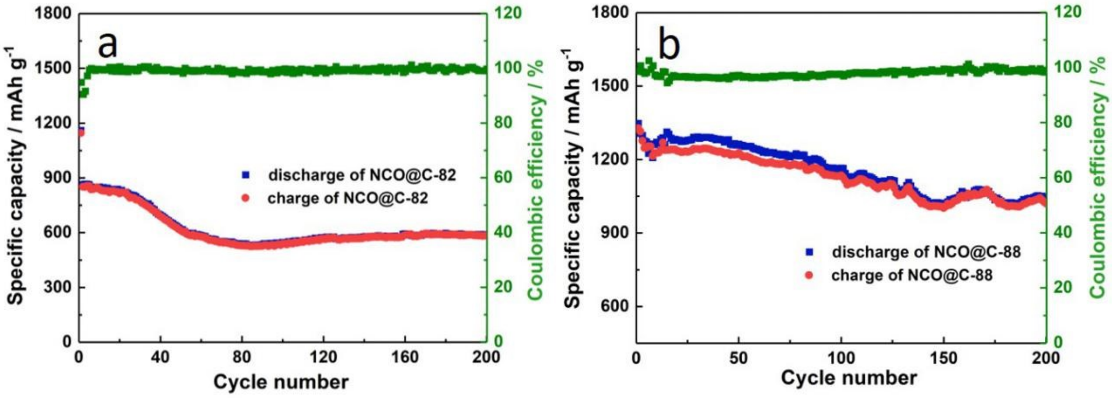

Fig. S6 Cycling performance of NCO@C-82 (a) and NCO@C-88 (b) composite nanofibers

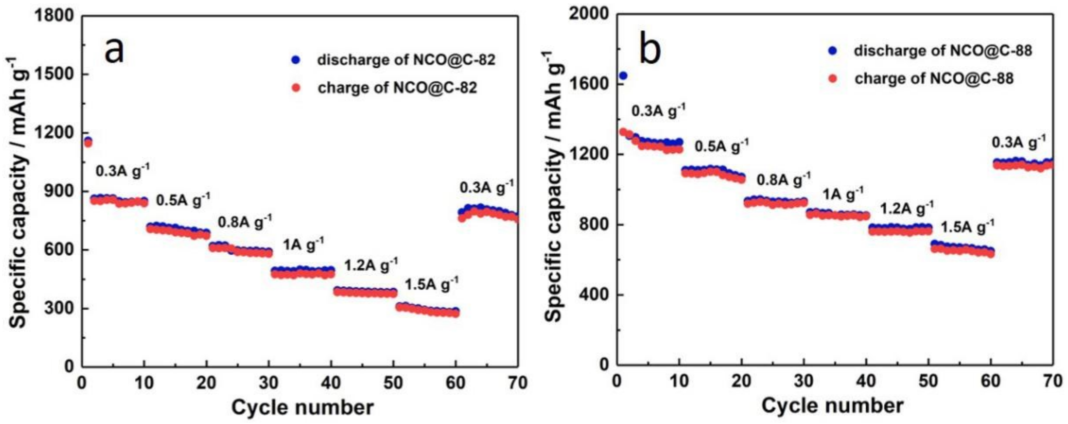

Fig. S7 Rate performances of NCO@C-82 (a) and NCO@C-88 (b) composite nanofibers

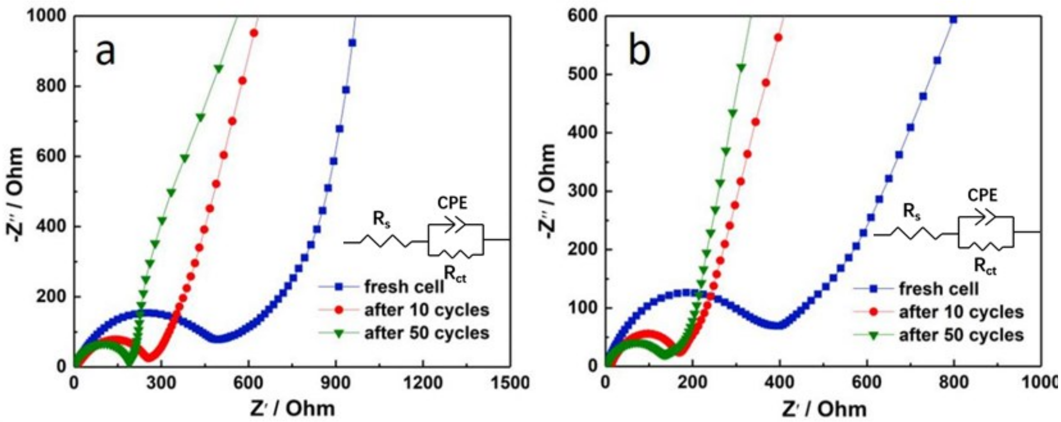

Fig. S8 Electrochemical impedance spectra and equivalent circuit model of NCO@C-82 (a) and NCO@C-88 (b) composite nanofibers

Rate performance of NCO@C-82 and NCO@C-88 electrodes:

The capacities of NCO@C-82 nanofibers (**Fig. S7a**) were only 850, 688, 591, 496 and 385 mAh g^{-1} when increasing the current density from 0.3 to 1.2 A g^{-1}. And the capacity decreased to 286 mAh g^{-1} at 1.5 A g^{-1}, which even inferior to that of graphite (372 mAh g^{-1}). However, when the current density reverted to 0.3 A g^{-1}, the capacity returned to 772 mAh g^{-1} as well. By contrast, the rate performance of NCO@C-88 nanofibers (**Fig. S7b**) was much better than that of NCO@C-82, the capacity retention of 1270, 1072, 933, 853, 783, 650 and 1158 mAh g^{-1} corresponding to the current densities of 0.3, 0.5, 0.8, 1, 1.5, 2 and 0.3 A g^{-1}, respectively. It was worth noting that the NCO@C-86 nanofibers maintained stable capacity at every stage and delivered much higher reversible capacity than NCO@C-46, NCO@C-82 and NCO@C-88 nanofibers.

Electrochemical impedance spectra of NCO@C-82 and NCO@C-88 electrodes:

The NCO@C-82 electrode (**Fig. S8a**) displayed resistances of 490 Ω, 255 Ω and 190 Ω before cycling, after 10 cycles and 50 cycles, respectively. The NCO@C-82 electrode showed resistance of 490 Ω before cycling, and the resistance dropped down to 255 Ω after 10 cycles, and 190 Ω after 50 cycles. By contrast, the resistance of NCO@C-88 (**Fig. S8b**) was much lower than that of NCO@C-82 before cycling (400 Ω), after 10 cycles (170 Ω) and 50 cycles (135 Ω). Although the same trend of decreasing resistance for NCO@C-46, NCO@C-82, and NCO@C-88 was presented after cycling, they were still higher than that of NCO@C-86 at the corresponding stage.

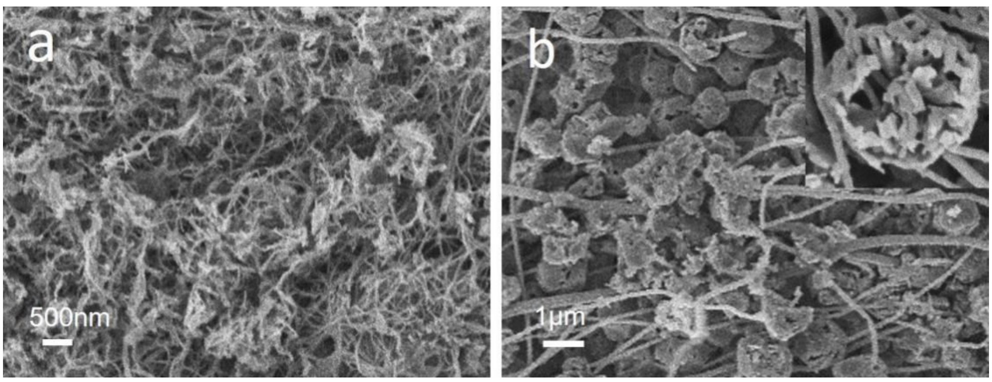

Fig. S9 SEM images of ZIF/PAN-Ni-82 (a) and NCO@C-88 (b) composite nanofibers after 200 cycles